MACF1 overexpression in BMSCs alleviates senile osteoporosis in mice through TCF4/miR-335–5p signaling pathway

Kewen Zhang [a,b,c,d], Wuxia Qiu [a,b,c,d,g], Hui Li [f], Jun Li [f], Pai Wang [a,b,c,d], Zhihao Chen [a,b,c,d], Xiao Lin [a,b,c,d,e,**], Airong Qian [a,b,c,d,*]

[a] Lab for Bone Metabolism, Xi'an Key Laboratory of Special Medicine and Health Engineering; Key Lab for Space Biosciences and Biotechnology, China
[b] School of Life Sciences, Northwestern Polytechnical University, Xi'an, Shaanxi, China
[c] Research Center for Special Medicine and Health Systems Engineering, School of Life Sciences, Northwestern Polytechnical University, Xi'an, Shaanxi, China
[d] NPU-UAB Joint Laboratory for Bone Metabolism, School of Life Sciences, Northwestern Polytechnical University, Xi'an, Shaanxi, China
[e] Research & Development Institute of Northwestern Polytechnical University in Shenzhen, Shenzhen City, 518063, China
[f] Department of Joint Surgery, Honghui Hospital, Xi'an Jiaotong University, Xi'an, Shaanxi, China
[g] School of Chemical Engineering, Sichuan University of Science & Engineering, Zigong, China

ARTICLE INFO

ABSTRACT

Background: The decreased osteogenic differentiation ability of mesenchymal stem cells (MSCs) is one of the important reasons for SOP. Inhibition of Wnt signaling in MSCs is closely related to SOP. Microtubule actin crosslinking factor 1 (MACF1) is an important regulator in Wnt/β-catenin signal transduction. However, whether the specific expression of MACF1 in MSC regulates SOP and its mechanism remains unclear.

Methods: We established MSC-specific Prrx1 (Prx1) promoter-driven MACF1 conditional knock-in (MACF-KI) mice, naturally aged male mice, and ovariectomized female mice models. Micro-CT, H&E staining, double calcein labeling, and the three-point bending test were used to explore the effects of MACF1 on bone formation and bone microstructure in the SOP mice model. Bioinformatics analysis, ChIP-PCR, qPCR, and ALP staining were used to explore the effects and mechanisms of MACF1 on MSCs' osteogenic differentiation.

Results: Microarray analysis revealed that the expression of MACF1 and positive regulators of the Wnt pathway (such as TCF4, β-catenin, Dvl) was decreased in human MSCs (hMSCs) isolated from aged osteoporotic than non-osteoporotic patients. The ALP activity and osteogenesis marker genes (Alp, Runx2, and Bglap) expression in mouse MSCs was downregulated during aging. Furthermore, Micro-CT analysis of the femur from 2-month-old MSC-specific Prrx1 (Prx1) promoter-driven MACF1 conditional knock-in (MACF-cKI) mice showed no significant trabecular bone changes compared to wild-type littermate controls, whereas 18- and 21-month-old MACF1 c-KI animals displayed increased bone mineral densities (BMD), improved bone microstructure, and increased maximum compression stress. In addition, the ovariectomy (OVX)-induced osteoporosis model of MACF1 c-KI mice had significantly higher trabecular volume and number, and increased bone formation rate than that in control mice. Mechanistically, ChIP-PCR showed that TCF4 could bind to the promoter region of the host gene miR-335–5p. Moreover, MACF1 could regulate the expression of miR-335–5p by TCF4 during the osteogenic differentiation of MSCs.

Conclusion: These data indicate that MACF1 positively regulates MSCs osteogenesis and bone formation through the TCF4/miR-335-5p signaling pathway in SOP, suggesting that targeting MACF1 may be a novel therapeutic approach against SOP.

The translational potential of this article: MACF1, an important switch in the Wnt signaling pathway, can alleviate SOP through the TCF4/miR-335-5p signaling pathway in mice model. It might act as a therapeutic target for the treatment of SOP to improve bone function.

---

* Corresponding authorSchool of Life Sciences, Northwestern Polytechnical University, Xi'an, Shaanxi 710072, China.
** Corresponding authorSchool of Life Sciences, Northwestern Polytechnical University, Xi'an, Shaanxi 710072, China
  E-mail addresses: linxiao@nwpu.edu.cn (X. Lin), qianair@nwpu.edu.cn (A. Qian).

1. Introduction

Senile osteoporosis (SOP) is a metabolic bone disease that is primarily associated with advanced age and postmenopause in women. It is often characterized by low bone mass and destruction of bone microarchitecture, ultimately leading to increased bone fragility and thus susceptibility to fractures [1]. Due to the high global prevalence and disability of age-related osteoporosis, the World Health Organization (WHO) has ranked osteoporosis as one of the most important global public health problems after coronary heart disease [2]. With the accelerated population aging in China, it is expected that the population over 60 will account for 20% of the total population by 2025, so the prevention and treatment of age-related osteoporosis has become one of the important research areas in health medicine in China.

The decrease in osteogenic differentiation of MSCs with age leads to reduced bone formation, which is the main cause of osteoporosis in the elderly. It was found that the expression levels of the bone formation marker genes BGLAP and ALP were significantly reduced in the bone tissue of elderly patients with osteoporosis and were negatively correlated with age [3]. MSCs have the potential to self-renew and differentiate into osteoblasts, chondrocytes, adipocytes, etc. During bone formation, MSCs differentiate into osteoblasts and play an important role in the synthesis, secretion, and mineralization of bone matrix [4]. Several studies have shown that the use of small molecules as drugs can promote the number of osteoblasts and improve bone formation, which has become an effective treatment for osteoporosis in the elderly [5].

MACF1 (microtubule actin cross-linking factor 1), also known as ACF7 (actin cross-linking factor 7, can bind to actin filaments with its N-terminal calponin homology domain, and interact with microtubules with the C-terminal EF-hand/GAR domain [6–8]. MACF1 has been identified as a regulator in several biological processes such as cell growth, differentiation, and migration [9]. Importantly, the studies have established the role of MACF1 in the migration and the differentiation of osteoblast. The results suggest that a lack of MACF1 may suppress migration and differentiation in osteoblasts [10–12]. MACF1 promotes the translocation of β-catenin from the cytosol to the cell membrane, where it is released and enters the nucleus forming a complex with TCF/LEF proteins to activate the Wnt target gene transcription. These results demonstrate that MACF1 is a positive regulator of the Wnt signaling pathway [13]. The Wnt/β-catenin signaling pathway is critical for the regulation of bone formation and bone metabolic diseases [14], which promotes bone formation by regulating the expression of osteogenic differentiation-specific genes. Furthermore, it has been shown that the inhibition of Wnt/β-catenin activation leads to reduced bone formation in mice [15]. Several studies have revealed that the development of age-related osteoporosis is associated with inhibition of the Wnt pathway in MSCs [16] and that the expression of Wnt-related proteins and the nuclear translocation capacity of β-catenin show a negative correlation with age [17,18]. However, it is not clear whether MACF1 is involved in the regulation of osteogenic differentiation in age-related osteoporosis.

MiRNAs play an important role in the regulation of stem cell differentiation fate, and their expression is spatiotemporally regulated by key upstream regulators. MiR-335 is encoded by the second intron of its host gene, MEST [19], and can be co-transcribed with the MEST gene [20]. Recent studies have revealed that miR-335 plays a key role in osteogenic differentiation by regulating the stem cell differentiation switch as well as related signaling pathways. It was shown that miR-335 expression is upregulated during early osteogenic differentiation of MSCs and is regulated by Runx2/Dicer [21] and promotes osteogenic differentiation of mouse MSCs by targeting DKK1 (dickkopf-related protein 1), an inhibitor of the Wnt signaling pathway [22]. Schoeftner S et al. found that miR-335 regulates the key cell differentiation gene Oct4 and regulates cell self-renewal and cell cycle in mouse embryonic stem cells [23]. These studies suggest that miR-335-5p plays an important role in the regulation of cellular osteogenic differentiation. However, how miR-335-5p is regulated in age-related osteoporosis has not been elucidated.

In the current study, we investigated the role of MACF1 in regulating the osteogenic differentiation of MSCs and its effect on bone formation in age-related osteoporosis. The investigation showed that MACF1 overexpression in MSCs alleviated SOP progression by promoting bone formation. The mechanistic investigations revealed MACF1, as a positive regulator of the Wnt signaling pathway, promotes the expression of miR-335-5p through TCF4 transcription in MSCs and regulates MSCs osteogenic differentiation through the TCF4/miR-335-5p pathway.

2. Materials and methods

2.1. Gene expression profile

Gene expression profile data were mined from the NCBI Gene Expression Omnibus (GEO, ncbi. nlm.nih.gov/geo/) database (GSE35959 and GSE74209). These datasets contained data on the expression profile of human MSCs (hMSCs) from aging and primary osteoporosis patients. Analysis was performed using the series matrix file in the database. For multiple probes of the same gene, the maximum value was used as the gene expression value.

2.2. Cell preparation

Mouse primary MSCs were isolated from the compact bones of male Rosa26-Macf1$^{f/f}$ and Rosa26-Macf1$^{f/f}$/Prx1-Cre mice. Briefly, the femora were isolated, cleaned, and transferred to a 60-mm-dish containing α-MEM supplemented with 2% (v/v) FBS (Corning, cat. no.35-081-CV) and 0.1% (v/v) penicillin (Sigma, cat. no.4687)/streptomycin (Sigma, cat. no, 1277). Epiphyses at both ends were cut and bone marrow was removed. The cortical bone was cut into pieces and digested by 1 mg/mL (w/v) Type II collagenase for 1 h at 37°C. Bone slides were washed with PBS and then collected and seeded in a 60-mm dish and incubated at 37°C in an incubator with 5% CO_2. Growth medium (α-MEM supplemented with 10% (v/v) FBS, 1% (v/v) penicillin-streptomycin, 1% (v/v) L-glutamine) was changed every three days to remove loosely attached cells and tissue debris. Cells in passages 2-5 were used for experiments. The induction medium containing α-MEM supplemented with 10% (v/v) FBS, 1% (v/v) penicillin-streptomycin, 1% (v/v) L-glutamine, 0.1 μM dexamethasone, 50 μg/mL (w/v) ascorbic acid, and 10 mM β-glycerophosphate was used for osteogenic induction.

2.3. ALP staining

Alkaline phosphatase (ALP) staining was performed using a BCIP/NBT alkaline phosphatase color development kit (Beyotime, Shanghai, China) following the manufacturer's instructions. Briefly, cells were washed with cold PBS, fixed in 4% polyformaldehyde (PFA) for 20 min, and then washed. The working solution was prepared by mixing BCIP (5-Bromo-4-chloro-3-indolyl phosphate) and NBT (nitro blue tetrazolium chloride) into a color development buffer, and cells were then stained in the dark for 15 min. Stained cells were scanned using a digital scanner (CanoScan 9000 F MarkII, Tokyo, Japan).

2.4. Rosa26-Macf1$^{f/f}$/Prx1-Cre mice generation

Prrx1-Cre (Prx1-Cre) and Rosa26-Macf1$^{flox/flox}$ (Rosa26-Macf1$^{f/f}$) mice were used in the current study. Prx1-Cre mice were crossed with Rosa26-Macf1$^{f/f}$ mice, and their progeny was bred to obtain MSC-specific conditional knock-in mice (Rosa26-Macf1$^{f/f}$/Prx1-Cre, cKI). Rosa26-Macf1$^{f/f}$ (flox) mice served as the control. The genotypes were identified by isolating DNA from the toes or tails of newborn mice and amplifying it by PCR. PCR was conducted in a BIO-GENER GE4852T thermocycler (BIO-GENER, Hangzhou, China) with an initial denaturation at 95°C for 5 min; then 35 cycles at 95°C for 30 s, 55°C for 30 s, 72°C for 30 s; and a final round at 72°C for 10 min. 1% agarose gels (HydraGene, R9012LE,

Piscataway, NJ) stained with 0.1% GoldView (Hat Biotechnology, Hangzhou, China) were used to visualize the PCR products. The sequences of the primers used for genotyping have been listed in Table 1.

3. Animal models

3.1. Senile osteoporotic mice model

All C57BL/6 mice were purchased from the Laboratory Animal Center of Air Force Medical University (Xi'an, Shaanxi, China) and were maintained on a 12-h light/dark cycle with free access to water and standard laboratory food. All animal experiments were performed by the Guiding Principles for the Care and Use of Laboratory Animals, and all experimental procedures were approved by the Institutional Experimental Animal Committee of Northwestern Polytechnical University (Xi'an, Shaanxi, China).

Naturally aged male mice of different ages were used as senile osteoporotic mouse models. The health of mice was monitored throughout their development until they were 18- and 21-month-old. The unhealthy mice were excluded.

3.1.1. Ovariectomized mice model

The 6-month-old female C57BL/6 J mice were ovariectomized (OVX) and then euthanized at 15 months of age. Make sure there are more than 6 mice in each group. Bone specimens (bilateral femurs/tibias and vertebrae) and blood samples from control and OVX mice were collected. Osteoporosis in OVX mice was confirmed by micro-CT analysis before further investigation.

3.1.2. Micro-CT analysis

To visualize the bone microarchitecture, fixed femur samples were scanned by a micro-CT device (SkyScan1276, Bruker, Billerica, MA, US). Briefly, femur tissues were isolated and fixed in 4% PFA. The fixed samples were then secured to the sample holder and scanned by the micro-CT device at an isotropic resolution of 10 μm (Energy: 70 kV, 114 μA; angle of increment: 0.2°; exposure time: 810 ms per frame; and scanning time: 14 min), and images were acquired using built-in software. The region of interest was selected 1 mm above the distal growth plate. All data was 3D-reconstructed using NRecon Reconstruction Software v1.7.1.6 (Micro Photonics Inc., Allentown, PA, US) and analyzed by CTAn Software v1.17.9.0 (Blue Scientific Ltd., Cambridge, UK) and CTvox Software v3.3.0.0 (Blue Scientific Ltd.). The values for bone mineral density (BMD), bone volume fraction (bone volume per tissue volume, BV/TV), trabecular thickness (Tb.Th.), trabecular number (Tb.N.), trabecular separation (Tb.Sp) and structure model index (SMI) were quantified to evaluate trabecular microarchitecture.

3.1.3. Histochemical, and histomorphometric analysis

PFA-fixed, paraffin-embedded tissue sections were prepared and stained using conventional methods. Briefly, fresh tissue was fixed in 4% PFA, decalcified in 10% EDTA, dehydrated through graded ethanol, and embedded in paraffin. Sections were taken at a depth of 4 μm. H&E was performed on serial sections. Stained sections were then scanned using a digital slide scanner (Aperio AT2, Leica, Wetzlar, Germany). For histomorphometric parameters, images were analyzed using the Histomorph Suite and Image-Pro Plus (Media Cybernetics, Rockville, MD, USA).

3.1.4. Three-point bending test

The mechanical properties of the bone and compressive strength of the tibia mid-diaphysis were examined by a three-point bending mechanical test system (UniVert, Canada). The tibias were prepared for a bio-mechanical test by wrapping them in saline-soaked gauze. The distance between two lower support points was 8 mm. Using the UniVert mechanical test system, a flexion moment was applied in the anteroposterior plane of the surface at a constant displacement rate of 0.6 mm/min until 0.5 mm of displacement occurred during three-point bending. The mechanical data were acquired and used to determine the maximum load, stiffness, and elasticity modulus.

3.1.5. Double calcein labeling

15-month-old mice were injected intraperitoneally with calcein (10 mg/kg, Sigma cat. no.c0875) 10 and 2 days before euthanasia. Femora were then collected, fixed, and embedded in graded methyl methacrylate after conventional tissue dehydration and cleaning. 20-μm-thick sections were obtained using the EXAKT 300CP tissue cutting systems and stained using a modified Goldner's trichrome staining method. Slides were visualized using a phase contrast microscope (BIOQUANT OSTEO-SCAN, Nashville, TN, USA). Bone dynamic histomorphometric analyses for mineral apposition rate were performed with image analysis software (ImageJ; National Institutes of Health, Bethesda, MD).

3.1.6. RNA-seq sample preparation

Total RNAs were extracted using the single-step acid guanidinium thiocyanate-phenol-chloroform method [24] with modifications. In brief, tissues were pulverized by fine grinding in liquid nitrogen and transferred to an ice-chilled guanidinium thiocyanate mix. After incubation on ice for 5 min, the solution was centrifuged at 4°C to obtain RNA-containing supernatant, which was then precipitated using ethanol, washed, and dissolved in DEPC-treated water. RNAs were washed 2 more times by phenol-chloroform before being checked for purity and integrity by agarose gel electrophoresis and quantified by determining the absorbance at 260 nm on SmartSpec (Bio-rad).

3 μg of total RNA was used for cDNA library preparation with the Balancer NGS Library Preparation Kit for small/microRNA (GnomeGen) following the manufacturer's instructions. Briefly, RNAs were ligated to 3′ and 5′ adaptors sequentially, reverse transcribed to cDNA, and amplified by PCR. The whole library was run on 10% native PAGE gel

Table 2
Primer sequences for ChIP-PCR.

Primer		Sequence	Product size
MEST	Forward	5′ TGGGAAAGGATACATTTGATTAGG3′	84bp
	Reverse	5′ ATTACTCATCAAAGGCACCAGG 3′	
MEST-1	Forward	5′ TAGGAGGCAACCCAAATCAC3′	72bp
	Reverse	5′ TCTGCCACAGCAGGATTTTC3′	

Table 1
Primer sequences for genotyping.

Primer	Sequence		Product size
Rosa-GT	Forwards	5′-AGTCGCTCTGAGTTGTTATCAG3′	WT:469bp
	Reserve	5′-TGAGCATGTCTTTAATCTACCTCGATG3′	
Rosa-MACF1-Mut	Forwards	5′-GACCTCTTAGAGACGCAGTCTGC3′	Mut:395bp
	Reserve	5′-CTCCTCATAAAGAGACAGCAACCAG3′	
Prrx1-Cre-WT	Forwards	5′-AGCGTTTGGTGTTGATTCGAGC3′	WT:267bp
	Reserve	5′-AGTCCCGGTGACTCCAGCAG3′	
Prrx1-Cre-Mut	Forwards	5′-AGCGTTTGGTGTTGATTCGAGC3′	Mut:322bp
	Reserve	5′-GGCTTGCAGGTACAGGAGGTAG3′	
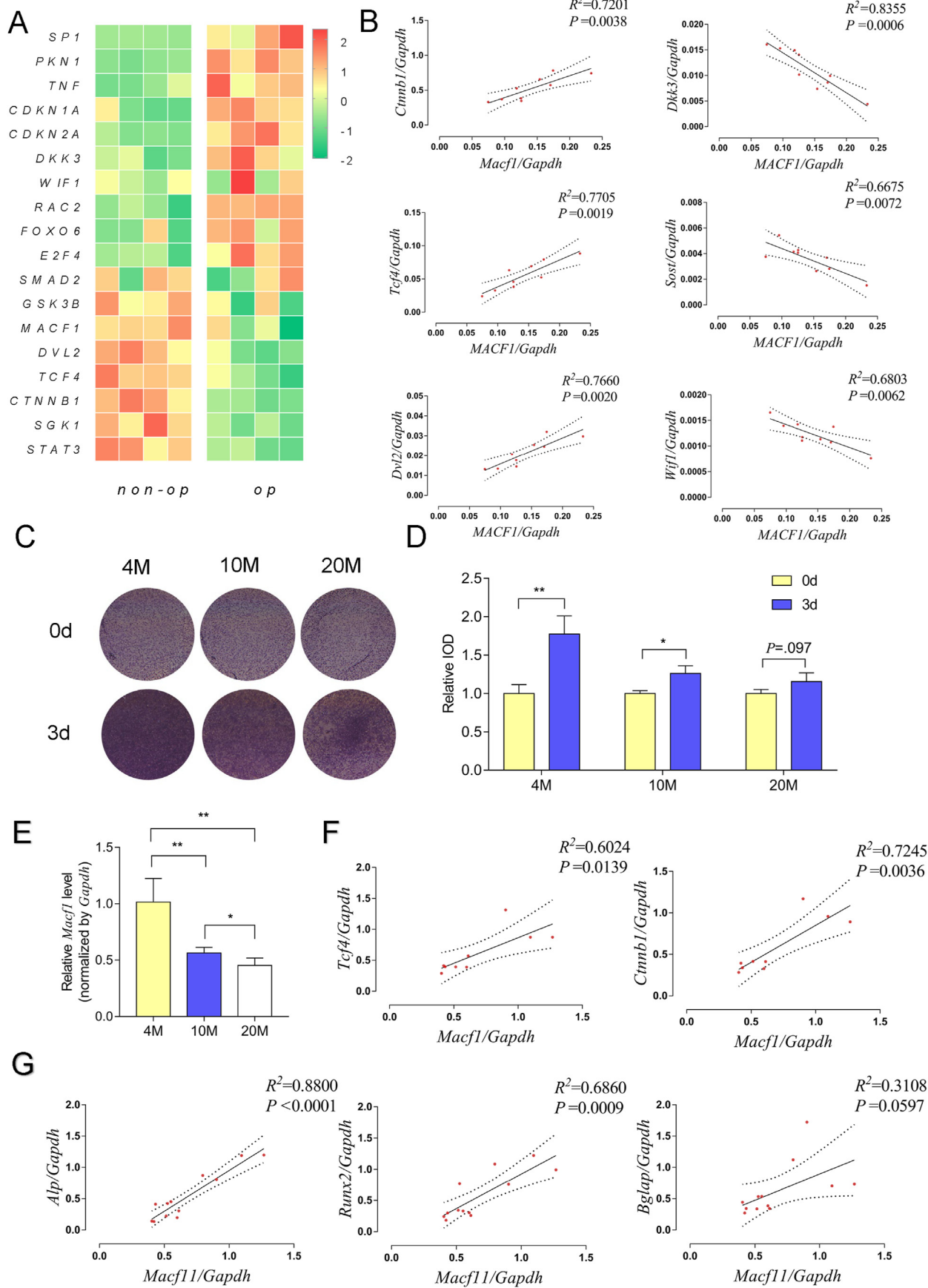
(caption on next page)

Figure 1. Correlation between MACF1 and Wnt signaling pathway in SOP
(A), Gene expression profile of MSCs from elderly, and elderly osteoporotic patients (GSE35959) **(B)**, Correlation analysis between Macf1 levels and levels of Wnt related gene in MSCs from elderly and elderly osteoporosis patients **(C)**, ALP staining and of MSCs of 4-, 10- and 20-month male C57BL/6 mice **(D)**, Quantification of relative integrated optical density (IOD) values of ALP staining using Image-Pro Plus 6.0 software (mean ± SD, *P < .05 **P < .01) **(E)**, Expression of MACF1 in MSCs of 4-,10- and 20-month male C57BL/6 mice, respectively, as detected by RT-PCR (mean ± SD, *P < .05 **P < .01) **(F)** Correlation analysis between Macf1 levels and levels of β-catenin and TCF4 in MSCs of 4-, 10- and 20-month male C57BL/6 mice **(G)**, Correlation analysis between Macf1 levels and levels of Alp, Runx2, and Bglap in MSCs of 4-,10-and 20-month male C57BL/6 mice.

electrophoresis, and bands corresponding to microRNA insertion were cut and eluted. After ethanol precipitation and washing, the purified small RNA libraries were quantified with a Qubit Fluorometer (Invitrogen) and submitted to the Illumina NextSeq 500 system for 151 nt pair-end sequencing by ABlife. Inc (Wuhan, China).

3.1.7. RNA isolation and real-time quantitative PCR

High-quality total RNA from cell and tissue samples was isolated using the TRIzol™ reagent according to the manufacturer's instructions. RNA quality was determined by ultraviolet spectrophotometry, and cDNA was synthesized from 1 μg of total RNA using the cDNA synthesis kit (TaKaRa, Kusatsu, Japan) following the manufacturer's instructions. Real-time quantitative PCR was performed using the SYBR Green method using 2 μL cDNA in a 20 μL PCR system. PCR data were analyzed with the comparative CT method ($2^{-\triangle\triangle CT}$). Gapdh was used as the internal control.

3.1.8. Western blot

To extract protein from bones, femora were excised, flash-frozen, and pulverized into bone chips using a mortar and pestle in the presence of liquid nitrogen (soft tissues were pulverized using a tissue pulverizer (PRIMA PB100-SP08, London, UK), and then digested with protein lysis buffer (Beyotime P0013, supplemented with protease inhibitor cocktail). The lysate was then centrifuged at 12,000 g for 2 min, and the supernatant was collected. For Western blot analysis, protein samples separated by SDS-PAGE were transferred onto a PVDF membrane and probed with antibodies against target proteins. Briefly, 20 μg protein samples were electrophoresed at 100 V on 5% stacking gel and 10% separating gel. After transfer onto a PVDF membrane (100 V, 90 min) and incubation with 5% non-fat milk for 30 min, the membrane was probed with primary antibodies against MACF1 and GAPDH. Washed membranes were then incubated with HRP-conjugated secondary antibodies, and developed and imaged (Gel Doc™ XR + Gel System). MACF1 antibody was obtained from Novus (Colorado, USA), Gapdh antibody was obtained from Proteintech (Chicago, USA) and antibodies for DKK1 and Bglap were purchased from Santa Cruz Biotechnology (Texas, USA).

3.1.9. Cell transfection

MSCs were seeded at a cell density of 2×10^4 cells/cm^2 and transfected with 30 nM si-TCF4 by Lipofectamine 3000 (Invitrogen, USA). After transfection for 6 h, the serum-free medium was replaced by a growth medium. Cells were harvested for real-time PCR, Western blot analysis, and ALP staining after 48 h. The si-TCF4 (Gene Pharma, China) sequence was 5′-GACGACAAGAAGGAUAUCATT-3'. The efficiency of TCF4 knockdown in MSCs is over 70%.

3.1.10. Chromatin immunoprecipitation

10^7 MSC cells were collected and fixed with 37% formaldehyde. 1.25 M Glycine was added to neutralize the reaction after 10 min. The cells were then scraped and centrifuged with $1 \times$ PBS containing $1 \times$ protease inhibitor cocktail to obtain protein precipitation. TCF4/TCF7L2 antibody (Invitrogen ChIP grade, catalog number MA5-14935) was used to obtain DNA fragments that bind to TCF4. Quantitative PCR was performed using the primers in the promoter region of the mouse gene MEST. Primer sequences are presented in Table 2.

3.2. Statistical analyses

Statistical analysis was performed using GraphPad PRISM 5.0. All results are expressed as mean ± SD. A Student's *t-tests* were performed to assess the statistical significance of differences. For all experiments, significance was defined as *P < 0.05 and **P < 0.01.

4. Result

### 4.1. Correlation between MACF1 and Wnt signaling pathway in SOP

To investigate the interaction between Macf1 and Wnt signaling-related genes in SOP, we analyzed the transcriptome of hMSC from 3 patients (79–94 years old) suffering from osteoporosis (OP) with 3 patients in the control group (79–89 years old, non-OP) (Fig. 1A). Genome-wide gene expression patterns were examined through microarray hybridizations, and the obtained data were compared by the SAM method (GEO accession number GSE35958). The NCBI database was used for genome-wide association studies, meta-analysis, and candidate gene association studies. We observed enhanced expression of negative regulators of the Wnt signaling pathway such as WIF, SOST, and DKK3 and reduced expression of Macf1, Dvl, β-catenin and TCF4, which are known to positively regulate the Wnt signaling pathway, in the OP group compared to non-OP group. In addition, the correlation analysis of gene expression in patients with osteoporosis showed that Macf1 expression was positively related to the activation of the Wnt signaling pathway (Fig. 1B).

We further verified the expression of Macf1 and Wnt-related genes during osteogenic differentiation of MSCs isolated from mice of different ages. After osteogenic induction, MSCs from 4-, 10-, and 20-month-old mice were stained for ALP. We observed declined ALP activity with age (Fig. 1C–D). Furthermore, the expression of osteogenic genes (Alp, Runx2, and Bglap) was significantly decreased in the elderly mice (Fig. 1E), accompanied by downregulation of Macf1, β-catenin, and TCF4 (Fig. 1F). These data suggest that decreased osteogenic ability is closely related to the down-regulated expression of MACF1 and Wnt-related genes in SOP.

4.2. Overexpression of MACF1 in MSCs does not affect bone mass in young mice

To verify the effect of Macf1 expression in MSCs on bone formation in SOP we utilized Cre/LoxP technology to construct a genetically modified mouse model in which the MACF1 gene was inserted into the Rosa26 locus in mesenchymal cells (Fig. 2A–C). We then tested Macf1 expression in primary MSCs to verify whether the Macf1 gene was specifically knocked in using real-time PCR and Western blot analyses. The results showed significantly increased expression of Macf1 in MSCs from cKI mice (Rosa-MACF1$^{f/f}$; Prx1$^{Cre/+}$, cKI) compared to littermate mice (Rosa-MACF1$^{f/f}$; Prx1$^{+/+}$, flox) (Fig. 2D). The organ-specific expression of Macf1 in bone tissue was confirmed through real-time PCR by comparing it with other tissues (heart, lung, and kidney) (Fig. 2E). The results of micro-CT and H&E staining showed no significant differences in bone mineral density, trabecular volume, trabecular thickness, or bone microarchitecture in 3-month-old male cKI mice compared with littermate flox mice (Fig. 2F–I). By observing the state and phenotype of the
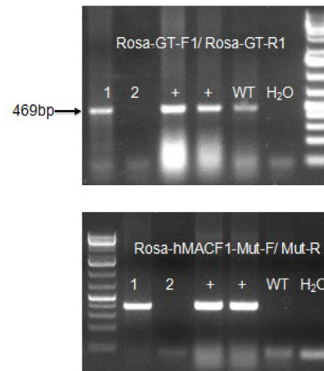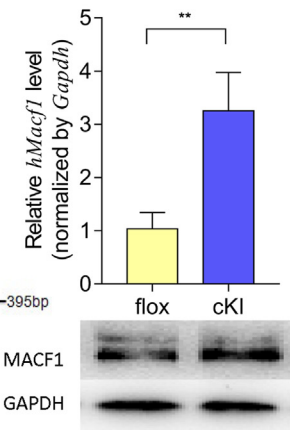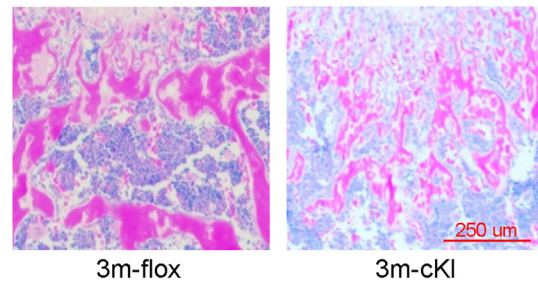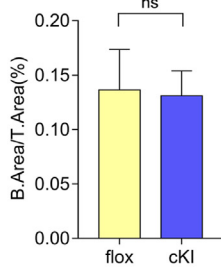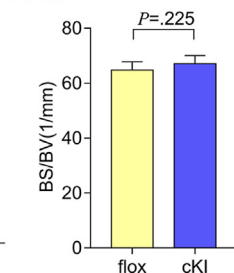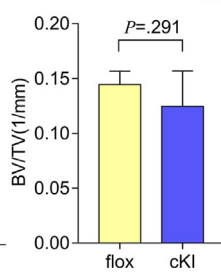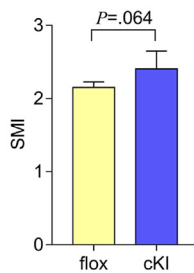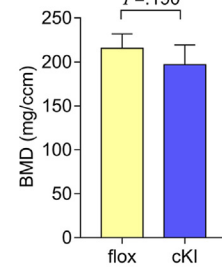
A Wild type ROSA26 allele
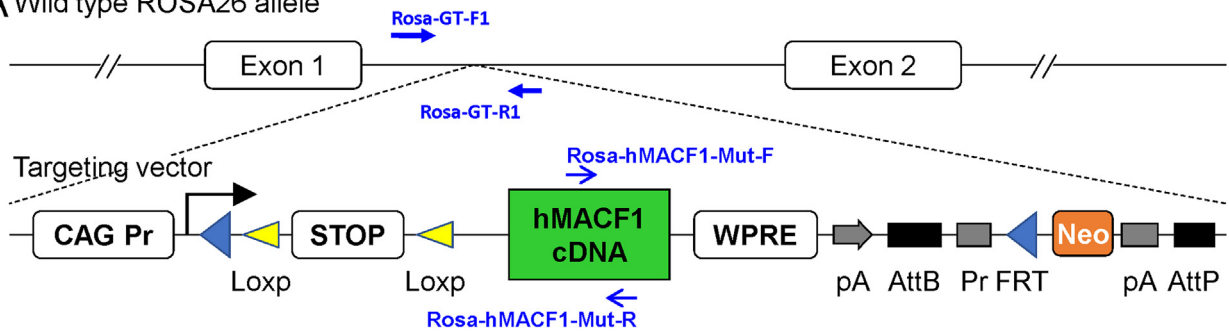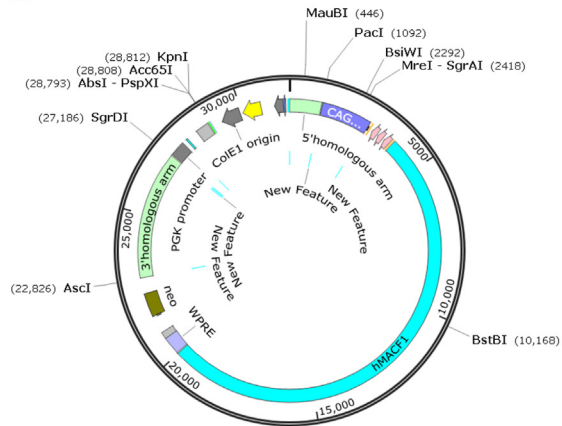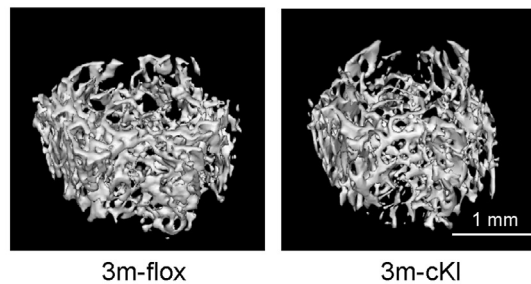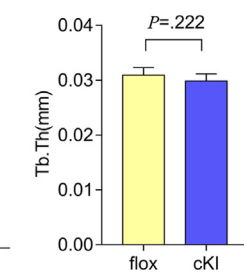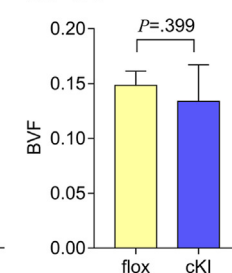
(caption on next page)

Figure 2. Genotyping and phenotyping of MACF1 over-expressed mice in MSCs **(A)**, Schematic illustration of the wild-type Rosa26 allele **(B)**, Map of hMACF1 targeting Vector for ROSA26 site knocking-in **(C)**, PCR genotyping images of ROSA26-MACF1$^{f/+}$ mice (1#). f, ROSA-MACF1 allele carrying loxP sites; +, ROSA26 allele **(D)**, The mRNA and protein expression of Macf1 in primary MSCs obtained from bone marrow of 2-month ROSA-Macf1$^{f/f}$ and ROSA-Macf1$^{f/f}$ Prx1-Cre mice were measured by qPCR and Western blot **(E)**, The mRNA expression of Macf1 in tibia, heart, lung and kidney of ROSA26-MACF1$^{f/f}$ and ROSA26-MACF1$^{f/f}$Prx1-cre mice were measured by qPCR **(F)**, Representative HE staining images of femur from 3-month-old ROSA26-MACF1$^{f/f}$ and ROSA26-MACF1$^{f/f}$Prx1-cre mice. The boxed area was magnified to show the trabecular bone **(G)**, Quantification of bone area/tissue area in HE staining images of femur from 3-month-old ROSA26-MACF1$^{f/f}$ and ROSA26-MACF1$^{f/f}$Prx1-cre mice **(H)**, Micro computed tomography (µCT) examination was performed to determine the bone formation in 3-month murine femurs **(I)**, Quantification data of bone mineral density (BMD), Structure Model Index (SMI), bone volume/tissue volume (BV/TV), and trabecular bone thickness (Tb. Th) in G. All data are presented as mean ± SD, n = 6, NS denotes not significant. f/f denotes ROSA26-MACF1$^{f/f}$; f/f/cre denotes ROSA26-MACF1$^{f/f}$Prx1-cre;

mice, we found that cKI mice could survive normally and had normal phenotypes with no noticeable changes in their behavior. Therefore, we speculate that MACF1 may regulate osteogenic differentiation in MSC and bone formation in aging mice.

4.3. Overexpression of MACF1 alleviates bone degenerative phenotype caused by SOP

Therefore, we employed mice of different ages to explore the regulatory effects of MACF1 on bone tissue structure and mechanical properties. Trabecular bone from 18- and 21-month-old flox and cKI mice were used to determine the structural parameters by micro-CT analysis (Fig. 3A). The result showed that the bone mass and volume of the distal femur of cKI mice were significantly higher than those of flox mice at 18 and 21 months of age. Flox mice had fewer bone trabeculae, and the microstructure of the trabeculae deteriorated during aging. It is worth noting that, with increased age, BMD has a disparity between flox and cKI mice, which was increased from 17.7% (18-month-old) to 44.2% (21-month-old). In 18- and 21-month-old flox mice, BV/TV and TB.N declined by 41.8% and 42.1%, respectively. In contrast, there was no significant change in cKI mice. Therefore, these results suggest that MACF1 improved bone mass in aged mice (Fig. 3B).

In addition, the result of the three-point bending test showed no significant difference in the flox and cKI group at age of 18 months. However, we found increased maximum compression stress, compression strain, and Young's elasticity modulus in the femur of cKI group mice at the age of 21 months, suggesting that Macf1 strengthened the toughness and strength of the bone in cKI mice during the aging process (Fig. 3D). Therefore, these results suggest that mesenchymal expression of MACF1 positively regulates bone mass and bone mechanical properties, and overexpression of MACF1 reduces the risk of a bone degenerative phenotype caused by SOP.

4.4. Overexpression of MACF1 reduces the adverse effects of menopause on bone

We next investigated whether overexpression of MACF1 could rescue post-menopausal osteoporosis. 6-month-old flox and cKI mice were ovariectomized. The establishment of OVX-induced osteoporosis was confirmed after 9 months of surgery. The results of micro-CT showed a significant decrease in bone volume and trabeculae number in flox mice after OVX (Fig. 4A). The BV/TV and TB.N declined by 57.3% and 52.8%, respectively, whereas the cKI group showed a decline of 37.8% and 32.8%, respectively. The above results show that after OVX, the bone volume and trabeculae number in cKI mice were significantly higher than in flox mice. Furthermore, quantification of the trabecular bone separation (TB. SP) and pattern factor (TB. PF) showed improved bone microarchitecture (Fig. 4B).

Calcein double labeling was used to examine the bone formation at the distal femur, revealed a greater distance between two labeled mineralization fronts in trabecular bone form cKI mice compared to flox in both the sham and OVX groups (Fig. 4C). In addition, the dynamic bone marker mineral attachment rate (MAR) was 43% higher in cKI-OVX than in flox-OVX groups (Fig. 4D). These data suggest that the overexpression of MACF1 in MSCs could promote bone formation and thus mitigate the adverse effects of menopause on bone mass.

### 4.5. MACF1 regulates the expression of miR-335–5p by TCF4 transcription in MSCs

MACF1, as a positive regulator of the Wnt signaling pathway, is involved in the regulation of multiple transcription factors, and it may regulate the expression of various miRNAs, which have been reported to act as modulators of gene expression affecting various cellular behaviors. Therefore, we first compared the miRNA expression profiles of bone tissues from the OP and non-OP groups (GSE74209). This analysis identified a subset of 49 SOP-related miRNAs whose absolute value of log fold change was larger than 1.5 and whose adjusted *p*-value was below 0.05 (Fig. 5A). Furthermore, we knocked down MACF1 in MC3T3-E1 and induced these cells by osteogenic induction medium for 0, 3, 5, and 10 days. The miRNA expression profiles of the samples were then analyzed by miRNA array. We observed 8 key differentially expressed miRNAs associated with osteoblastic differentiation which have been shown in the heatmap (Fig. 5B) [25]. The miRNAs were further analyzed by an online web server: The miRNA Enrichment Analysis and Annotation Tool (https://ccb-compute2.cs.uni-saarland.de/mieaa2/) [26] which showed that miR-335-5p was associated with the Wnt pathway. Therefore, we analyzed the expression of miR-335-5p in MSCs isolated from mice of different age groups (Figs. 5C) and 60- and 90-year-old patients (Fig. 5D). The expression of miR-335-5p in MSCs from SOP patients and mice in different age groups was detected by real-time quantitative PCR. We detected down-regulation of miR-335-5p with increasing age, which is consistent with MACF1 expression in MSCs.

Preliminary experiments have established that the expression of TCF4, an important transcription factor downstream of the Wnt signaling pathway, is positively correlated with MACF1. Literature research found that miR-335-5p is encoded by intron 2 of MEST, which is identified to be expressed in mesodermal tissues and known as a mesoderm-specific transcript [27]. The expression levels of miR-335-5p significantly correlated with those of MEST, supporting the notion that the intronic miR-335 is co-expressed with its host gene [28]. Thus, the online transcription factor binding site prediction tool, PROMO, was used to analyze the promoter regions of MEST/miR-335-5p [29]. The prediction results of PROMO show that TCF4, which is closely related to MACF1 expression and as an important downstream TFs of the Wnt pathway, may bind to the promoter region of miR-335-5p. The sequence logo of TCF4 and two TCF4 binding sites (−2938 to −2862, −1492 to −1411) were identified in the promotor region of MEST (−3000 to +100) by JASPAR (https://jaspar.genereg.net/) (Fig. 5E) [30]. The ChIP assay was performed using an anti-TCF4 antibody. The agarose gel electropherogram image showed that DNA was pulled down by an anti-TCF4 antibody (Fig. 5F), indicating that TCF4 binds to the MEST promoter region (−2938 to −2862, −1492 to −1411). These results suggest that MACF1 may regulate the expression of miR-335-5p through TCF4 transcription in MSCs.
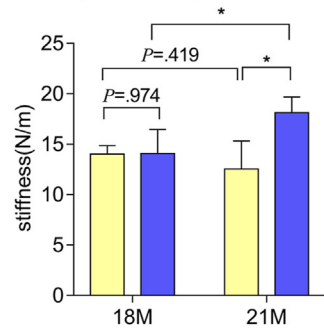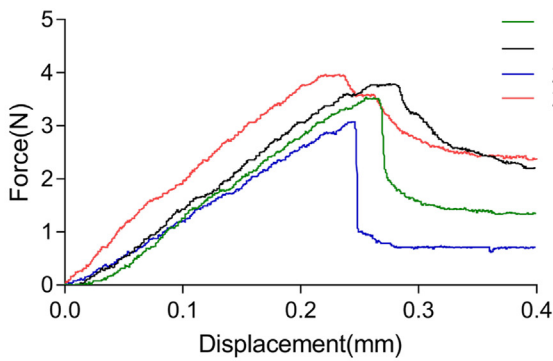
4.6. MACF1 regulates MSCs osteogenic differentiation through TCF4/miR-335–5p signaling pathway

To elucidate whether MACF1 could regulate the expression of miR-335-5p by TCF4, we knocked down TCF4 in MSCs using siRNA. The qPCR results showed that the overexpression of MACF1 promoted the expression levels of TCF4 and miR-335-5p. Inhibition of TCF4 resulted in
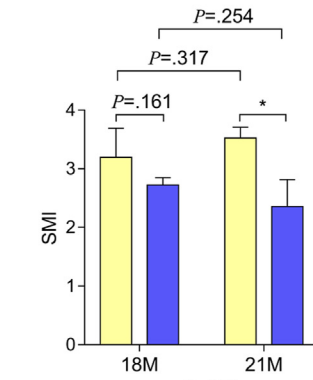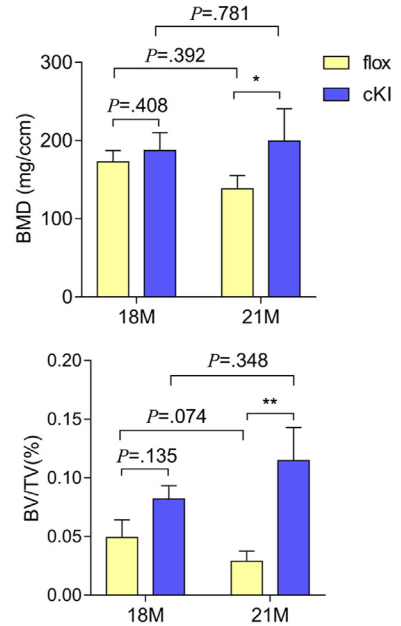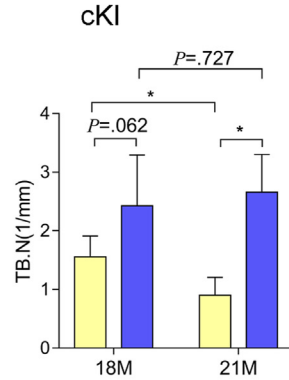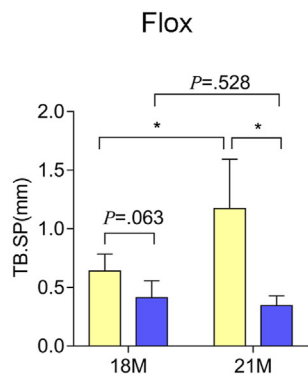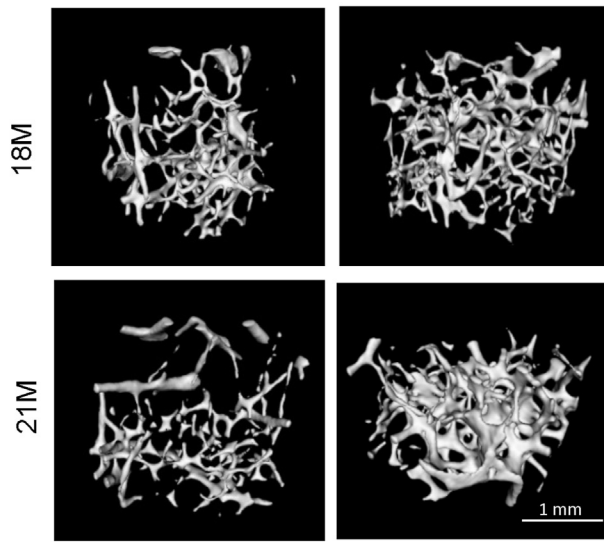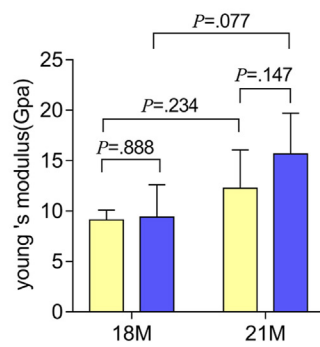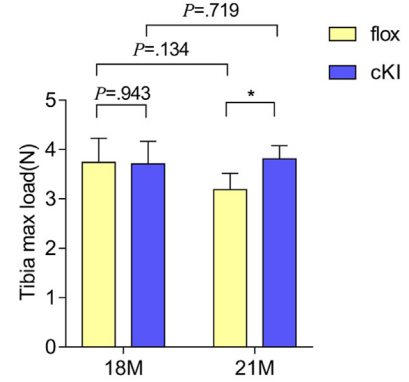
Figure 3. Overexpression of MACF1 benefits bone mass and bone mechanical properties in SOP **(A)**, Micro computed tomography (μCT) examination was performed to determine the bone formation in 18-and 21-month murine femurs **(B)**, Quantification data of bone mineral density (BMD), Structure Model Index (SMI), trabecular bone thickness (Tb. th), trabecular bone numbers (Tb.N), bone volume/tissue volume (BV/TV), bone surface/bone volume (BS/BV), trabecular separation (Tb. Sp), and bone volume fraction (BVF) in A. All data are presented as mean ± SD, n = 6, NS denotes not significant, *P < .05, **P < .01 **(C)**, Representative load-deflection curves for the respective groups, and three-point bending measurement of tibia max load in 18- and 21-month-old mice **(D)**, Biomechanical properties of fracture load, Young's modulus, and stiffness in tibia of 18-and 21-month-old ROSA26-MACF1$^{f/f}$ and ROSA26-MACF1$^{f/f}$Prx1-cre mice. Tibia (n = 6 per group). Data are presented as means ± SEM. *P < .05.

a significant decrease in the levels of miR-335-5p in both the flox and cKI groups (Fig. 6A). Furthermore, we measured the ALP activity and the expression of BGLAP by ALP staining (Fig. 6B–C), Western blot (Fig. 6D) and qPCR (Fig. 6E), respectively, to find out whether MACF1 could regulate osteogenic differentiation of MSCs through TCF4/miR-335-5p. The results showed that overexpression of MACF1 improved ALP activity, which was reduced by the inhibition of TCF4, and significantly decreased BGLAP expression in both the flox and cKI groups. In contrast, the expression of DKK1, which has been reported as a target gene of miR-335-5p, was up-regulated (Fig. 6D–E).

To further verify that MACF1 regulates the expression level of miR-335-5pby TCF4, we examined the expression of TCF4 and miR-335–5p in the primary MSCs of MACF1 cKO mice. These cKO mice were constructed from previous work in our lab [11]. The results showed significantly decreased TCF4 and miR-335-5p expression in the cKO group (Fig. 6F). These data indicate that MACF1 regulates osteogenic differentiation by regulating the levels of miR-335-5p by TCF4.

5. Discussion

There has been an increasing interest about the function of MACF1 in regulating MSCs' osteogenic differentiation in age-related osteoporosis. This study discovered that MACF1 overexpression in MSCs slowed SOP progression by promoting bone formation. More importantly, we demonstrated that MACF1 regulates MSC osteogenic differentiation by promoting the expression of miR-335-5p by TCF4 in MSCs.

Firstly, we explored the role of MACF1 in age-related osteoporosis. The bioinformatics analysis revealed that MACF1 was significantly reduced in the age-related osteoporosis group. Moreover, the expression of MACF1, Wnt-related genes, and osteogenic differentiation-related genes was decreased in the MSCs isolated from the aging patients. Expression of MACF1 in mice of different months demonstrated the negative correlation between MACF1 and age. In the previous research of our group, we found a mechanoresponsive miRNA, miR-138-5p, which directly targeted MACF1 and cause the downregulated MACF1 [31]. The increasing aging process inevitably leads to an increase in miR-138-5p expression and a decrease in mechanical stimulation, which might be one of the reasons for the decrease in MACF1 expression. These data suggest the potential role of MACF1 in the differentiation of MSCs in age-related osteoporosis. However, the upstream genes regulating MACF1 expression remain to be explored.

In previous studies, Hu et al. have reported that MACF1 regulates bone formation in a concentration-dependent manner [32]. Moreover, a deficiency of MACF1 has been shown to impair early-stage bone development, delay bone ossification, and decrease bone mass in mice [10]. The work has shown that by overexpressing MACF1 in the skull, mouse calvarial thickness, mineral apposition rate, and osteogenic marker protein expression can be significantly enhanced [33]. Interestingly, there was no significant increase in bone mass in the early stage of cKI mice when MACF1 was overexpressed, which suggests that the ability of MACF1 to promote bone formation *in vivo* tends to be saturated under normal physiological conditions. In our study, we constructed two age-related osteoporosis mouse models and found that overexpression of MACF1 significantly mitigated the negative consequences of aging. The physiological role of MACF1 was further validated by overexpressing MACF1 in MSCs, which increased bone mass and enhanced bone formation in the age-related osteoporosis group. It is well known that

osteoporosis and other bone diseases occur because multicellular communication within the basic multicellular unit is disrupted [34]. Yin et al. and our groups have reported that transfection of pEGFP-C1-ACF7 plasmid in MACF1 KD pre-osteoblasts could partially rescue bone loss caused by MACF1 deletion. However, no significant improvement in bone mass was found in MACF1 cKI mice, and this suggests that overexpression of MACF1 under normal conditions may have enhanced the osteogenic differentiation of MSCs, while the increase in osteoblasts also led to an increase in RANKL-induced mature osteoclasts. Lin et al. found that MACF1 knockdown inhibits RANKL-induced osteoclastogenesis [35]. And it suggests that, in cKI-aged mice, MACF1 overexpression in MSCs led to increased osteogenic differentiation, but MACF1 expression was reduced in osteoblasts and RANKL-induced osteogenic differentiation was inhibited. Under normal physiological conditions, a unilateral increase in the osteogenic differentiation capacity of MSCs may lead to an increase in bone resorption, ultimately manifesting as no significant change in bone mass. However, With the increasing aging process, both bone formation and bone resorption capacity diminish. By overexpression of MACF1 in MSCs, only the osteogenesis was enhanced. Thus, a net bone mass accumulation is observed due to increased bone formation.

Chen et al. and our groups have previously reported that MACF1 is a positive regulator that participates in the regulation of Wnt/β-catenin signaling [13,36]. Through bioinformatics analysis, we found the expression of TCF4, a downstream gene of the Wnt/β-catenin signaling pathway was positively correlated with MACF1 expression in age-related osteoporosis. Additionally, ChIP and promoter analysis revealed that TCF4 directly binds to the MEST promoter to regulate miR-335-5p expression. Besides, the miR-335-5p expression level was upregulated by the overexpression of MACF1, which also increased the TCF4 expression in the primary MSCs from cKI mice.

Recent studies have shown that high expression of miR-335-5p in both MSCs-derived and derived from mature dendritic cells can promote osteogenic differentiation of MSCs [37–39]. Lin et al. have reported that a positive feedback loop for miR-335–5p expression: miR-335-5p→DKK1→Wnt/β-catenin/TCF→Mest/miR-335-5p in MSCs [40]. We further found that MACF1 regulates the expression of miR-335–5p by TCF4, which affects the osteogenic differentiation ability of MSC. Through literature research, miR-335-5p has been extensively studied in fracture and bone restoration, and the results have shown that miR-335-5p has a positive effect on osteogenic differentiation. This suggests that miR-335 -5p plays an important role in osteogenic differentiation.

It is worth noting that, in the study of miR-335-5p, Zhang et al. found miR-335-5p promoted osteogenic differentiation *in vitro* by activating the Wnt/β-catenin signaling pathway through DKK1 downregulation [22]. Consistent with the *in vitro* study of Zhang et al., DKK1 protein expression was downregulated, whereas the β-catenin level was increased in bones of miR-335-5p overexpressed mice. As a key protein in the Wnt pathway, β-catenin plays a different role during MSC development. Hill and colleagues found the high β-catenin level at an early stage could prevent MSC from entering the prechondro-osteoblast lineage [41]. Once the MSC become prechondro-osteoblast precursors, a high β-catenin level is needed to promote osteogenesis as well as to prevent chondrogenesis. In this study, the MACF1 overexpression was under the control of Prx1-Cre, and no significant increase in bone mass was observed in three-month-old cKI mice under normal physiological conditions. This
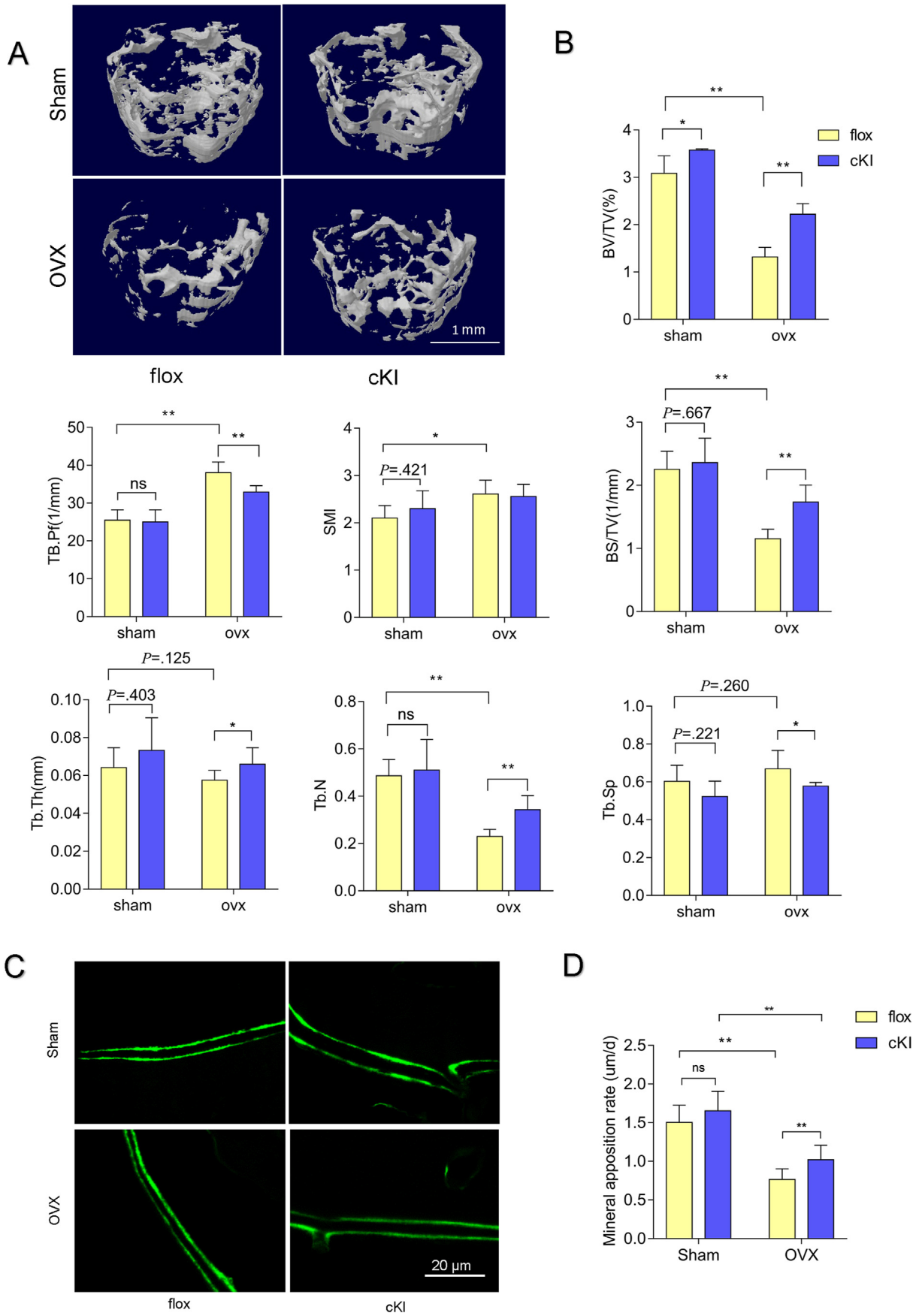
(caption on next page)

Figure 4. Overexpression of MACF1 reduces the adverse effects of menopause on bone

(A), Micro computed tomography (μCT) examination was performed to determine the bone formation in ovariectomized murine femurs **(B)**, Quantification data of bone volume/tissue volume (BV/TV), bone surface/tissue volume (BS/TV), bone surface/bone volume (BS/BV), Structure Model Index (SMI), trabecular bone thickness (Tb. th), trabecular bone numbers (Tb. N), trabecular separation (Tb. Sp), and trabecular bone pattern factor (Tb. pf) in A. All data are presented as mean ± SD, n = 6, NS denotes not significant, *P < .05, **P < .01 **(C)**, Representative fluorescent images of calcein double labelling of femur from sham and ovariectomized ROSA26-MACF1 ^f/f and ROSA26-MACF1^f/f Prx1-cre mice showing increased bone mineralization in trabecular bone **(D)**, Quantification of mineral apposition rate in femur of sham and ovariectomized ROSA26-MACF1 ^f/f and ROSA26-MACF1^f/f Prx1-cre mice. All data are presented as mean ± SD, n = 6, NS denotes not significant, **P < .01;
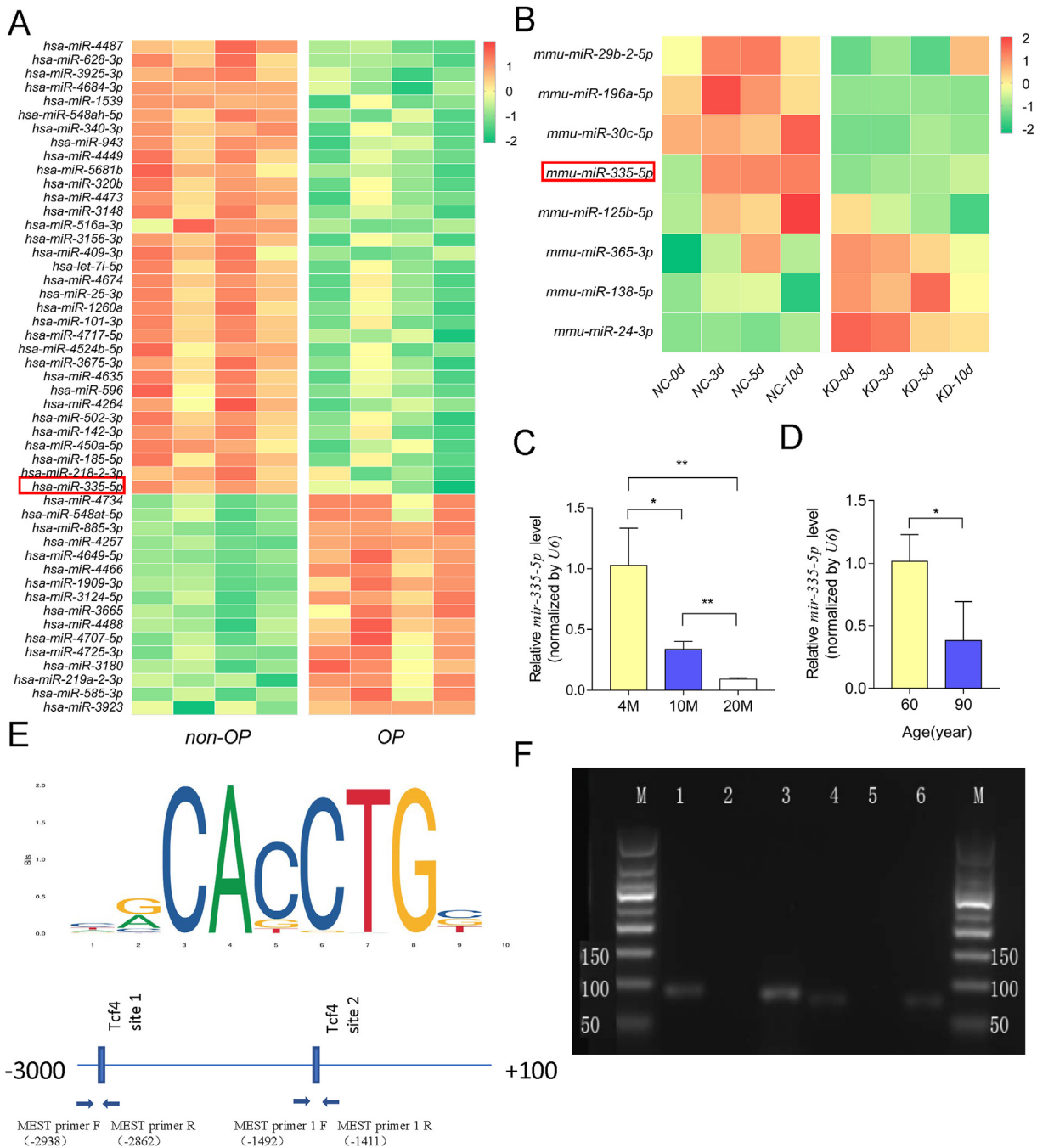

Figure 5. MACF1 promotes the expression of miR-335-5p through TCF4 transcription in MSCs

(A), Heat map showing the osteogenic related miRNAs from the bone tissue of elderly, and elderly osteoporotic patients (GSE74209) **(B)**, Heat map showing miRNAs with significant differences in control and MACF1-KD cells, during osteogenic differentiation **(C)**, Expression of mir-335 in MSCs of 4-, 10- and 20-month male C57BL/6 mice respectively, as detected by RT-PCR (mean ± SD, *P < .05 **P < .01) **(D)**, Expression of mir-335 in MSCs of different aged (60 and 90) people respectively, as detected by RT-PCR (mean ± SD, **P < .01) **(E)**, The sequence logo of TCF4 and schematic display of MEST promoter region (−3000 to +100): predicted TCF4-binding sites, and ChIP primers positions **(F)**, ChIP product agarose gel electropherogram image (qPCR Amplification of MEST (84bp) MSC Lane 1: IP, Lane 2: neg, Lane 3: Input; qPCR Amplification of MEST-1 (72bp) MSC Lane 4: IP, Lane 5: neg, Lane 6: Input).
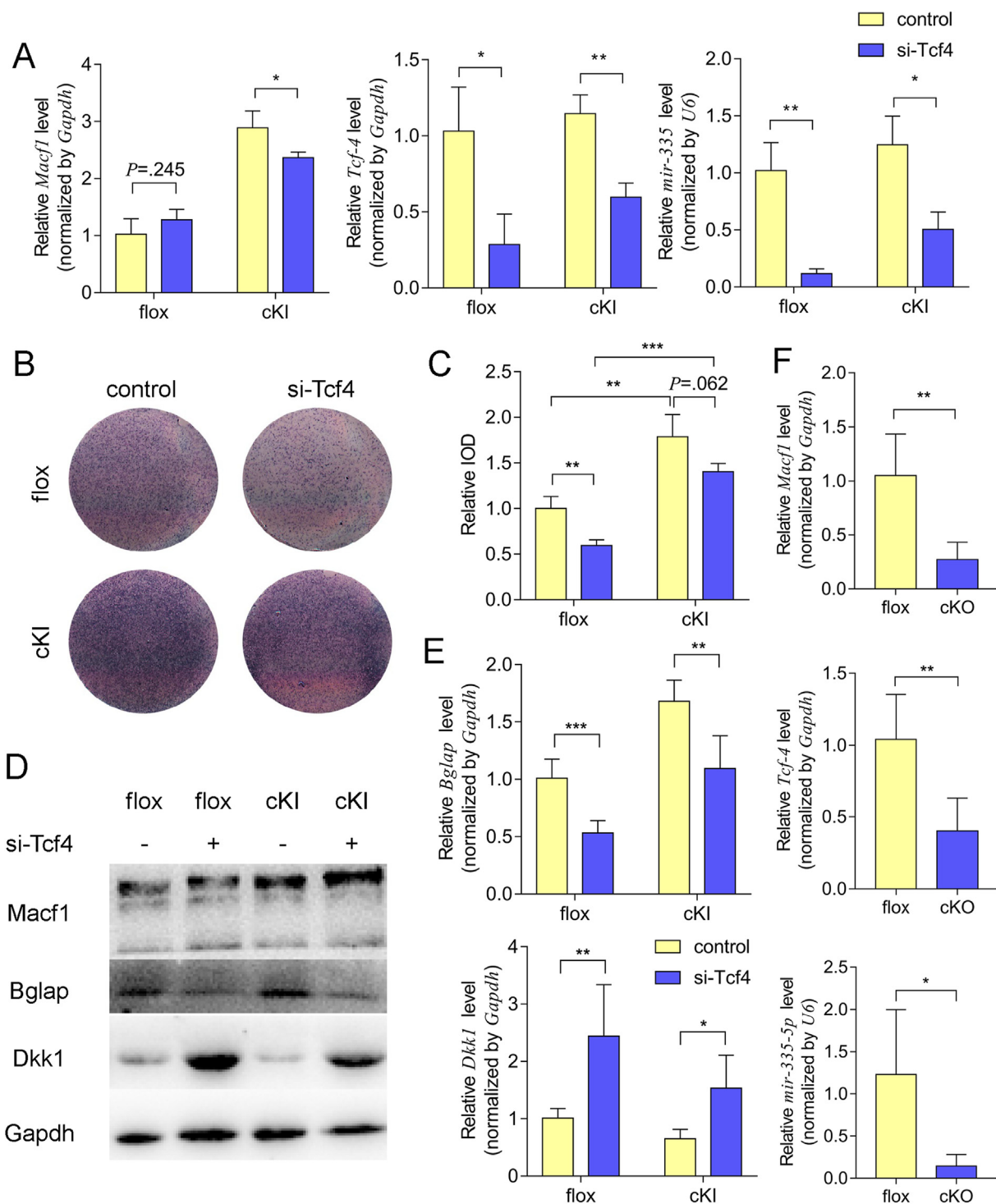
Figure 6. MACF1 regulates MSCs osteogenic differentiation through TCF4/miR-335

(A), Expression of MACF1, TCF4 and mir-335 in MSCs of ROSA26-MACF1$^{f/f}$ and ROSA26-MACF1$^{f/f}$Prx1-cre mice, as detected by RT-PCR (mean ± SD, *$P < .05$ **$P < .01$). MSCs were treated with or without TCF4 siRNA (siTCF4) **(B)**, ALP activity of MSCs from ROSA26-MACF1 $^{f/f}$ and ROSA26-MACF1$^{f/f}$Prx1-cre mice was detected by ALP staining. MSCs were treated with or without TCF4 siRNA (siTCF4) **(C)**, Quantification of relative integrated optical density (IOD) values of ALP staining using Image-Pro Plus 6.0 software (mean ± SD, *$P < .05$ **$P < .01$, ***$P < .001$) **(D–E)**, Expression of BGLAP and DKK1 in MSCs of ROSA26-MACF1$^{f/f}$ and ROSA26-MACF1$^{f/f}$Prx1-cre mice, as detected by Western blot and RT-PCR (mean ± SD, **$P < .01$, ***$P < .001$). MSCs were treated with or without TCF4 siRNA (si-TCF4) **(F)**, Expression of MACF1, Tcf4 and miR-335–5p in primary MSCs of MACF1 conditional knockout mice, as detected by RT-PCR (mean ± SD, *$P < .05$ **$P < .01$).

may indicate that the overexpression of MACF1 leads to high β-catenin expression by increasing the expression of miR-335-5p at the early stage in the development of cKI mice, which may prevent MSC becoming prechondro-osteoblast precursors but relatively increase the osteogenic differentiation potential of already differentiated from MSCs into osteoblast precursors. We observed with the advance of aging, the overall expression of β-catenin decreased, and the inhibitory effect of its high concentration on the differentiation of MSCs into prechondro-osteoblast

precursors was relieved. In aged cKI mice, the stable and high expression of MACF1, which is a positive regulator of the Wnt signaling pathway, promoted the expression of miR-335-5p. Furthermore, the stimulation of osteogenic differentiation of osteoblast precursors was maintained by the activated Wnt signaling pathway. Therefore, the phenotypes of enhanced bone formation were observed in the aging cKI mouse model, including increased bone mass and improved bone microarchitecture.

The differentiation process of MSCs is multi-stage and involves multiple signaling pathways. Consider the role of MACF1 in the Wnt signaling pathway, which was involved in regulating multiple transcription factors. Hu and Qiu et al. demonstrated that deficiency of MACF1 inhibited the expression of Runx2 in osteoblast [10,32]. Zheng et al. further determined the relationship between Runx2 and DICER [21]. DICER is the central enzyme that cleaves precursor microRNAs (miRNAs) into 21–25 nucleotide duplex and determines not only the fate of cell lineage differentiation, and identity, but also that of cell survival [42]. This indicates that MACF1 not only regulates the expression of miR-335-5p by TCF4 but is also involved in regulating the maturation of miR-335–5p. It suggests that MACF1 is an important skeleton protein that may participate and play different roles in multiple stages of miR-335-5p regulation.

6. Conclusion

Our study demonstrates for the first time that a high MACF1 level mitigates the negative consequences of aging, such as osteoporosis. Mechanistically, overexpression of MACF1 promotes miR-335-5p expression by upregulating TCF4, and miR-335-5p has been reported to promote osteogenic differentiation and bone formation. Our findings not only reveal a novel role and mechanism of MACF1 in SOP but also highlight the functions of MACF1 *in vivo*. Although the study significantly improve the understanding of role of MACF1 in bone formation in osteoporosis, more research will be required in the future to investigate the various functions of MACF1 overexpression in mice under aged and normal physiological conditions.

Declaration of competing interest

The authors declare that they have no known competing financial interests or personal relationships that could have appeared to influence the work reported in this paper.

References

[1] Li Y, Fan L, Hu J, Zhang L, Liao L, Liu S, et al. MiR-26a rescues bone regeneration deficiency of mesenchymal stem cells derived from osteoporotic mice. Mol Ther 2015;23(8):1349–57.

[2] An J, Yang H, Zhang Q, Liu C, Zhao J, Zhang L, et al. Natural products for treatment of osteoporosis: the effects and mechanisms on promoting osteoblast-mediated bone formation. Life Sci 2016;147:46–58.

[3] Wang X, Guo B, Li Q, Peng J, Yang Z, Wang A, et al. miR-214 targets ATF4 to inhibit bone formation. Nat Med 2013;19(1):93–100.

[4] Lin GL, Hankenson KD. Integration of BMP, Wnt, and notch signaling pathways in osteoblast differentiation. J Cell Biochem 2011;112(12):3491–501.

[5] Cosman F, Nieves J, Zion M, Woelfert L, Luckey M, Lindsay R. Daily and cyclic parathyroid hormone in women receiving alendronate. N Engl J Med 2005;353(6):566–75.

[6] Ma Y, Yue J, Zhang Y, Shi C, Odenwald M, Liang WG, et al. ACF7 regulates inflammatory colitis and intestinal wound response by orchestrating tight junction dynamics. Nat Commun 2017;8:15375.

[7] Kodama A, Karakesisoglou I, Wong E, Vaezi A, Fuchs E. ACF7: an essential integrator of microtubule dynamics. Cell 2003;115(3):343–54.

[8] Miao Z, Ali A, Hu L, Zhao F, Yin C, Chen C, et al. Microtubule actin cross-linking factor 1, a novel potential target in cancer. Cancer Sci 2017;108(10):1953–8.

[9] Hu L, Xiao Y, Xiong Z, Zhao F, Yin C, Zhang Y, et al. MACF1, versatility in tissue-specific function and in human disease. Semin Cell Dev Biol 2017;69:3–8.

[10] Qiu WX, Ma XL, Lin X, Zhao F, Li DJ, Chen ZH, et al. Deficiency of Macf1 in osterix expressing cells decreases bone formation by Bmp2/Smad/Runx2 pathway. J Cell Mol Med 2020;24(1):317–27.

[11] Zhao F, Ma X, Qiu W, Wang P, Zhang R, Chen Z, et al. Mesenchymal MACF1 facilitates SMAD7 nuclear translocation to drive bone formation. Cells 2020;9(3).

[12] Su P, Tian Y, Yin C, Wang X, Li D, Yang C, et al. MACF1 promotes osteoblastic cell migration by regulating MAP1B through the GSK3beta/TCF7 pathway. Bone 2022;154:116238.

[13] Chen HJ, Lin CM, Lin CS, Perez-Olle R, Leung CL, Liem RK. The role of microtubule actin cross-linking factor 1 (MACF1) in the Wnt signaling pathway. Genes Dev 2006;20(14):1933–45.

[14] Baron R, Kneissel M. WNT signaling in bone homeostasis and disease: from human mutations to treatments. Nat Med 2013;19(2):179–92.

[15] van Bezooijen RL, ten Dijke P, Papapoulos SE, Löwik CW. SOST/sclerostin, an osteocyte-derived negative regulator of bone formation. Cytokine Growth Factor Rev 2005;16(3):319–27.

[16] Shen L, Zhou S, Glowacki J. Effects of age and gender on WNT gene expression in human bone marrow stromal cells. J Cell Biochem 2009;106(2):337–43.

[17] Almeida M, Han L, Martin-Millan M, O'Brien CA, Manolagas SC. Oxidative stress antagonizes Wnt signaling in osteoblast precursors by diverting beta-catenin from T cell factor- to forkhead box O-mediated transcription. J Biol Chem 2007;282(37):27298–305.

[18] Manolagas SC, Almeida M. Gone with the Wnts: beta-catenin, T-cell factor, forkhead box O, and oxidative stress in age-dependent diseases of bone, lipid, and glucose metabolism. Mol Endocrinol 2007;21(11):2605–14.

[19] Kobayashi S, Kohda T, Miyoshi N, Kuroiwa Y, Aisaka K, Tsutsumi O, et al. Human PEG1/MEST, an imprinted gene on chromosome 7. Hum Mol Genet 1997;6(5):781–6.

[20] Tome M, Lopez-Romero P, Albo C, Sepulveda JC, Fernandez-Gutierrez B, Dopazo A, et al. miR-335 orchestrates cell proliferation, migration and differentiation in human mesenchymal stem cells. Cell Death Differ 2011;18(6):985–95.

[21] Zheng L, Tu Q, Meng S, Zhang L, Yu L, Song J, et al. Runx2/DICER/miRNA pathway in regulating osteogenesis. J Cell Physiol 2017;232(1):182–91.

[22] Zhang J, Tu Q, Bonewald LF, He X, Stein G, Lian J, et al. Effects of miR-335-5p in modulating osteogenic differentiation by specifically downregulating Wnt antagonist DKK1. J Bone Miner Res 2011;26(8):1953–63.

[23] Schoeftner S, Scarola M, Comisso E, Schneider C, Benetti R. An Oct4-pRb axis, controlled by MiR-335, integrates stem cell self-renewal and cell cycle control. Stem Cell 2013;31(4):717–28.

[24] Chomczynski P, Sacchi N. The single-step method of RNA isolation by acid guanidinium thiocyanate-phenol-chloroform extraction: twenty-something years on. Nat Protoc 2006;1(2):581–5.

[25] Huai Y, Zhang W, Chen Z, Zhao F, Wang W, Dang K, et al. A comprehensive analysis of MicroRNAs in human osteoporosis. Front Endocrinol 2020;11:516213.

[26] Kern F, Fehlmann T, Solomon J, Schwed L, Grammes N, Backes C, et al. miEAA 2.0: integrating multi-species microRNA enrichment analysis and workflow management systems. Nucleic Acids Res 2020;48(W1):W521–8.

[27] Yonekura S, Ohata M, Tsuchiya M, Tokita H, Mizusawa M, Tokutake Y. Peg1/Mest, an imprinted gene, is involved in mammary gland maturation. J Cell Physiol 2019;234(2):1080–7.

[28] Dohi O, Yasui K, Gen Y, Takada H, Endo M, Tsuji K, et al. Epigenetic silencing of miR-335 and its host gene MEST in hepatocellular carcinoma. Int J Oncol 2013;42(2):411–8.

[29] Messeguer X, Escudero R, Farré D, Núñez O, Martínez J, Albà MM. PROMO: detection of known transcription regulatory elements using species-tailored searches. Bioinformatics 2002;18(2):333–4.

[30] Castro-Mondragon JA, Riudavets-Puig R, Rauluseviciute I, Lemma RB, Turchi L, Blanc-Mathieu R, et al. JASPAR 2022: the 9th release of the open-access database of transcription factor binding profiles. Nucleic Acids Res 2022;50(D1):D165–73.

[31] Chen Z, Zhao F, Liang C, Hu L, Li D, Zhang Y, et al. Silencing of miR-138-5p sensitizes bone anabolic action to mechanical stimuli. Theranostics 2020;10(26):12263–78.

[32] Hu L, Yin C, Chen D, Wu Z, Liang S, Zhang Y, et al. MACF1 promotes osteoblast differentiation by sequestering repressors in cytoplasm. Cell Death Differ 2021;28(7):2160–78.

[33] Zhang Y, Yin C, Hu L, Chen Z, Zhao F, Li D, et al. MACF1 overexpression by transfecting the 21 kbp large plasmid PEGFP-C1A-ACF7 promotes osteoblast differentiation and bone formation. Hum Gene Ther 2018;29(2):259–70.

[34] Kular J, Tickner J, Chim SM, Xu J. An overview of the regulation of bone remodelling at the cellular level. Clin Biochem 2012;45(12):863–73.

[35] Lin X, Xiao Y, Chen Z, Ma J, Qiu W, Zhang K, et al. Microtubule actin crosslinking factor 1 (MACF1) knockdown inhibits RANKL-induced osteoclastogenesis via Akt/GSK3beta/NFATc1 signalling pathway. Mol Cell Endocrinol 2019;494:110494.

[36] Yin C, Zhang Y, Hu L, Tian Y, Chen Z, Li D, et al. Mechanical unloading reduces microtubule actin crosslinking factor 1 expression to inhibit beta-catenin signaling and osteoblast proliferation. J Cell Physiol 2018;233(7):5405–19.

[37] Zhang L, Tang Y, Zhu X, Tu T, Sui L, Han Q, et al. Overexpression of MiR-335-5p promotes bone formation and regeneration in mice. J Bone Miner Res 2017;32(12):2466–75.

[38] Cao Z, Wu Y, Yu L, Zou L, Yang L, Lin S, et al. Exosomal miR-335 derived from mature dendritic cells enhanced mesenchymal stem cell-mediated bone regeneration of bone defects in athymic rats. Mol Med 2021;27(1):20.

[39] Teng JW, Bian SS, Kong P, Chen YG. Icariin triggers osteogenic differentiation of bone marrow stem cells by up-regulating miR-335-5p. Exp Cell Res 2022;414(2):113085.

[40] Lin X, Wu L, Zhang Z, Yang R, Guan Q, Hou X, et al. MiR-335-5p promotes chondrogenesis in mouse mesenchymal stem cells and is regulated through two positive feedback loops. J Bone Miner Res 2014;29(7):1575–85.

[41] Tang CY, Chen W, Luo Y, Wu J, Zhang Y, McVicar A, et al. Runx1 up-regulates chondrocyte to osteoblast lineage commitment and promotes bone formation by enhancing both chondrogenesis and osteogenesis. Biochem J 2020;477(13):2421–38.

[42] Obernosterer G, Leuschner PJ, Alenius M, Martinez J. Post-transcriptional regulation of microRNA expression. RNA 2006;12(7):1161–7.